Successful Stabilization of Graphene Oxide in Electrolyte Solutions: Enhancement of Biofunctionalization and Cellular Uptake

Bong Jin Hong, Owen C. Compton, Zhi An, Ibrahim Eryazici, and SonBinh T. Nguyen*

Department of Chemistry, Northwestern University, 2145 Sheridan Road, Evanston, Illinois 60208-3113, United States

ABSTRACT

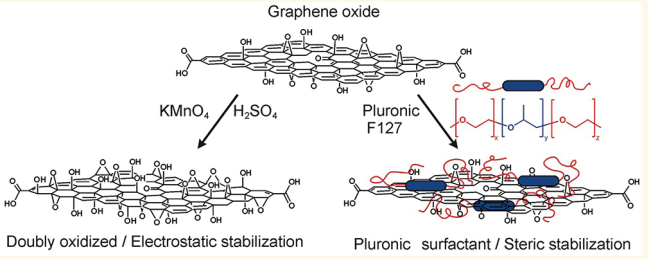

Aqueous dispersions of graphene oxide are inherently unstable in the presence of electrolytes, which screen the electrostatic surface charge on these nanosheets and induce irreversible aggregation. Two complementary strategies, utilizing either electrostatic or steric stabilization, have been developed to enhance the stability of graphene oxide in electrolyte solutions, allowing it to stay dispersed in cell culture media and serum. The electrostatic stabilization approach entails further oxidation of graphene oxide to low C/O ratio (∼1.1) and increases ionic tolerance of these nanosheets. The steric stabilization technique employs an amphiphilic block copolymer that serves as a noncovalently bound surfactant to minimize the aggregate-inducing nanosheet−nanosheet interactions. Both strategies can stabilize graphene oxide nanosheets with large dimensions (>300 nm) in biological media, allowing for an enhancement of >250% in the bioconjugation efficiency of streptavidin in comparison to untreated nanosheets. Notably, both strategies allow the stabilized nanosheets to be readily taken up by cells, demonstrating their excellent performance as potential drug-delivery vehicles.

KEYWORDS: graphene oxide · biofunctionalization · delivery vehicle · ionic stabilization · electrolytic stabilization · cellular uptake · Pluronics

Graphene oxide is a two-dimensional nanoparticle featuring a variety of chemically reactive functionalities, such as epoxy and hydroxyl groups on the basal plane and carboxylic acid groups along the sheet edge,[1,2] which can be differentially functionalized.[3,4] In spite of these surface moieties, a significant amount of the sp^2-hybridized carbon backbone structure remains intact,[5] allowing the nanosheet to retain a high degree of planarity, as demonstrated in thin-film deposition and fabrication experiments,[6,7] and a correspondingly high surface-to-volume ratio.[8] Together with these characteristics, the good biocompatibility of graphene oxide[9−11] suggests that it should be a promising material for biomedical applications such as drug delivery and biosensing. Indeed, several research groups have reported the modification of graphene oxide with proteins,[12−14] DNAs/RNAs,[15−18] or small drug molecules[10,19,20] and subsequent *in vitro* studies.[10,18,19,21]

Although the aforementioned studies have demonstrated the promise of graphene oxide in biological applications, a critical shortcoming of these nanosheets is their poor dispersity in electrolyte solutions, which must be addressed before their potential as a biomaterial platform can be fully realized. One can expect the oxygen-containing functional groups of graphene oxide, in addition to being chemical handles for functionalization, to also aid in solubilizing these nanosheets in nonionic aqueous and organic media.[22,23] However, this solubilization effect is weak and the nanosheets quickly aggregate when dispersed in electrolyte solutions, such as buffered saline.[10] Such aggregation behavior significantly limits the applicability of graphene oxide in biological applications, since they would lead to inefficient coupling with biomolecules, limited cellular uptake, and diminished delivery efficiency. The Dai group has circumvented this aggregation issue by utilizing *small* graphene oxide sheets (lateral dimensions <50 nm) that were covalently functionalized with amine-modified six-armed dendrimers of polyethylene glycol (PEG).[10] While this approach successfully allowed graphene oxide sheets to

* Address correspondence to stn@northwestern.edu.

Received for review June 26, 2011 and accepted October 23, 2011.

Published online October 23, 2011
10.1021/nn202355p

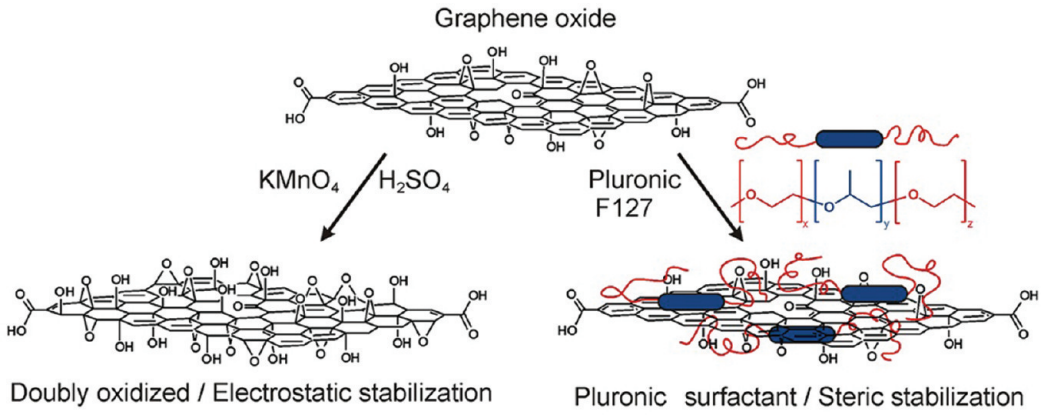

Figure 1. Schematic illustration of two complementary strategies for stabilizing graphene oxide in electrolyte solutions. Left: Further oxidation of graphene oxide nanosheets leads to enhanced electrostatic stabilization, Right: Pluronic F127 serves as a surfactant to sterically stabilize the graphene oxide nanosheets from aggregation.

be stabilized for cell studies, the material synthesis can be cumbersome at times.

Herein, we report two *complementary* methods for enhancing the dispersibility of amphiphilic[24] graphene oxide sheets in aqueous electrolyte solutions (Figure 1). The first approach entails further oxidation of graphene oxide to a low C/O ratio of 1.1, allowing it to be *electrostatically* stabilized in electrolyte solutions. This is the first instance, to the best of our knowledge, that graphene oxide has been dispersed in electrolyte solutions without any stabilizers, overcoming the limitations first reported by Li, Wallace, Kaner, and co-workers (that electrolytes aggregate graphene oxide dispersions).[25] In addition to having improved electrostatic stability and dispersibility in saline solutions, the resulting doubly oxidized graphene oxide material also possesses a plethora of chemically active sites that allow for enhanced biofunctionalization. The second strategy employs a commercially available triblock amphiphilic copolymer (Pluronic F127) as a *steric* stabilizer for the graphene oxide sheet. This copolymer features a central hydrophobic block of poly(propylene oxide) (PPO) that can associate with the unoxidized aromatic regions of the graphene oxide basal plane[5] and two flanking hydrophilic PEG arms[26,27] that provide steric stabilization in water. While amphiphilic copolymers such as Pluronic F127 have previously been used to stabilize *nonionic* aqueous dispersions of *graphene*,[26,28] we demonstrate herein that this block copolymer can also dramatically enhance the dispersity of *graphene oxide* in aqueous electrolyte solutions, which have been reported[25] to cause aggregation of graphene oxide dispersions. Using electrostatic and steric stabilization strategies, we establish, *beyond speculation*, that more efficient bioconjugation to graphene oxide and much better cellular uptake of the resulting biofunctionalized materials can indeed be achieved *via* either stabilization route. Our two complementary approaches provide simple and versatile means for enhancing the dispersion of graphene oxide in biological media, which subsequently lead to the superior cellular uptake of these stabilized nanosheets compared with untreated graphene oxide.

RESULTS AND DISCUSSION

While graphene and graphene oxide are both 2D nanosheets, the surface of graphene oxide features a significant number of oxygen-containing moieties, such as hydroxyl, epoxy, and carboxylic acid functional groups, distinctly differentiating it in chemical and physical properties from graphene. Among these differences, the excellent dispersibility of graphene oxide in water has been invoked as a justification for applying it to biological systems. Yet to date, this characteristic alone is not sufficient for delivery applications where stability in the presence of highly concentrated electrolytes is required. Of the few reports that have been published to date on the use of graphene oxide for biological delivery,[10,19,21] all have focused on the addition of stabilizers such as hydrophilic polymers or surfactants. While this is a sensible strategy, drawbacks include potential *in vivo* toxicity associated with the surfactant materials as well as a low payload limit attributed to the intrinsic steric hindrance that comes with surfactant usage. Thus, it would be highly advantageous if the dispersibility of graphene oxide sheets in aqueous electrolyte solutions could be increased without the need for surfactants.

Enhanced Electrostatic Stability by Further Oxidation of Graphene Oxide. As commonly prepared using the Hummers method, graphene oxide nanosheets typically exhibit a C/O ratio of <2, where a large number of epoxy and hydroxyl groups cover their basal planes and carboxylic acid moieties line up along their edges.[8] While these groups imbue negative charges that electrostatically stabilize graphene oxide in nonionic aqueous and organic media,[22,23] irreversible aggregation can be readily induced by introducing an electrolyte that can neutralize these surface charges.[25] Such is the case when dilute dispersions of as-prepared graphene

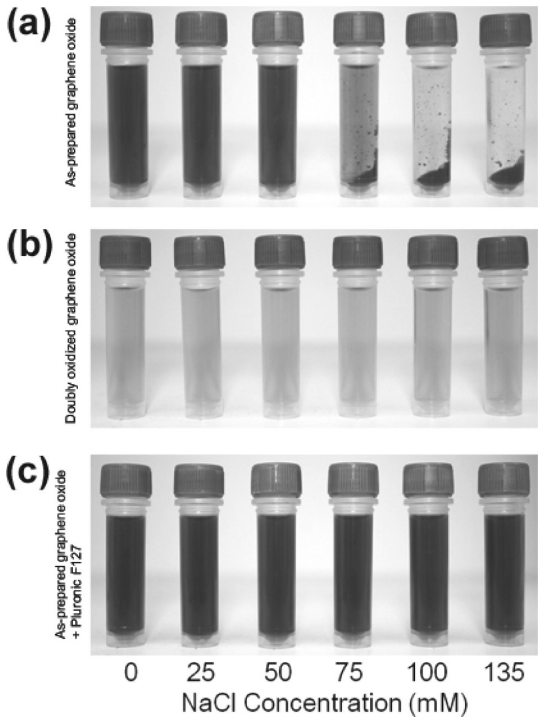

Figure 2. Digital images of solutions of (a) as-prepared graphene oxide (0.1 mg mL^{-1}) in the presence of NaCl, (b) doubly oxidized graphene oxide (0.1 mg mL^{-1}) in the presence of NaCl, and (c) as-prepared graphene oxide (0.1 mg mL^{-1}) in the presence of Pluronic F127 (1.0 mM) and NaCl. Images were recorded 5 min after the graphene oxide formulations were mixed with aqueous solutions containing increasing NaCl concentrations (from left to right: 0, 25, 50, 75, 100, and 135 mM final salt concentrations). Samples were briefly centrifuged (~30 s) to accentuate the aggregation of nanosheets into concentrated masses at the bottom of the tube, if any occurred. A color reproduction of this figure is available in the SI as Figure S1.

oxide (0.1 mg mL^{-1}, C/O ratio = 1.9) were suspended in aqueous salt solutions. Upon exposure to aqueous NaCl solution (final concentrations ≥75 mM), immediate precipitation of the graphene oxide could be observed visually (Figure 2a) and by dynamic light scattering (DLS) measurements (Figure S2 in the Supporting Information (SI)), which show a drastic conversion of the initially soluble, small (hydrodynamic diameters ~180 nm) graphene oxide sheets into larger (hydrodynamic diameters ~1.8 μm) aggregates. When the salt concentrations were ≥50 mM, extended exposure for 2 h completely aggregated the nanosheets (Figure S3 in the SI). However, at the lowest tested salt concentration (≤25 mM), a large amount of soluble graphene oxide species is still left in solution (Figure 2a and Figure S3 in the SI), suggesting that dispersions of as-prepared graphene oxide could tolerate small amounts of electrolyte.

Since aggregation of the negatively charged as-prepared graphene oxide nanosheets after exposure to electrolyte is presumably induced by electrolytic screening of the existing functional groups,[10,25] we hypothesize that highly oxidized graphene oxide sheets possessing even more anionic moieties along their edges should be better at resisting this screening. In addition, the increased presence of more oxygen-containing groups in highly oxidized graphene oxide, brought about at the expense of sp^2-hybridized graphitic domains on its basal plane, should also reduce aggregation-inducing attractive interactions between the graphene oxide sheets. Together, these two factors should increase the probability for highly oxidized graphene oxide sheets to remain well-dispersed in the presence of electrolytes. Such highly oxidized materials could be made by subjecting as-prepared graphene oxide to a second cycle of Hummers oxidation.[29] The resulting doubly oxidized graphene oxide exhibited a low C/O ratio of 1.1, corresponding to a ~70% increase in the oxygen content of the nanosheets. X-ray photoelectron spectroscopy (XPS) spectra before and after the second oxidation reveal corresponding significant increases in epoxy, hydroxyl, and carboxyl signals (Figure 3). Solid-state ^{13}C NMR (Figure S4 in the SI) and Fourier-transformed infrared (FTIR) (Figure S12 in the SI) spectra further confirm this observation: the intensity of signals due to oxygenated groups, primary contributors to electrostatic stabilization, increases significantly at the expense of the signal from graphitic carbons.[25] Consistent with the higher level of oxidation and further loss of sp^2-hybridized carbons, dispersions of these doubly oxidized sheets are lighter in color than the corresponding dispersions of as-prepared material (Figure S1 in the SI).

The electrostatic advantage gained *via* the second cycle of oxidation of the nanosheets is clearly demonstrated by a more negative zeta potential of the nanosheets (−60.6 ± 1.3 mV in contrast to −53.8 ± 2.4 in the as-prepared material). At NaCl concentrations as high as 135 mM, similar to the salt concentration in a 1× phosphate-buffered saline (PBS) media, the doubly oxidized graphene oxide exhibited excellent stability with no immediate aggregation observed (Figure 2b). Although some aggregation occurred after 2 h at NaCl concentrations ≥ 100 mM (Figure S3 in the SI), the doubly oxidized graphene oxide still exhibited outstanding stability in comparison with the as-prepared graphene oxide. This improved stability is most apparent in time-dependent DLS measurements, which showed the measured size of the doubly oxidized nanosheets (hydrodynamic radius ~200 nm, similar to that reported above for as-prepared graphene oxide) in electrolyte solution to remain nearly the same as that in water, even after incubation in 75 mM NaCl for 48 h (Figure S2 in the SI).

Although subjecting graphene oxide to a second cycle of oxidation significantly lowered its C/O ratio, the average size of the nanosheets does not change. Atomic force microscopy (AFM) measurement reveals that the average size of our doubly oxidized nanosheets (Figure S5 in the SI) is almost the same as that for

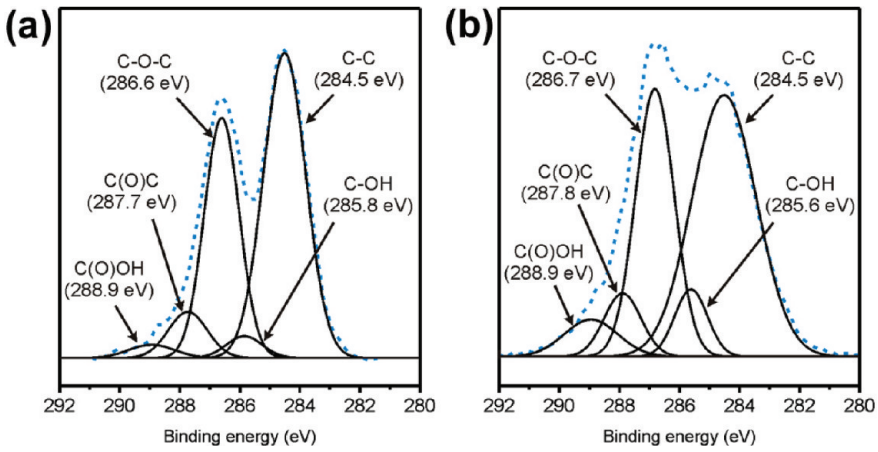

Figure 3. XPS spectra of (a) as-prepared and (b) doubly oxidized graphene oxide. The dashed lines represent the original data, while solid lines represent deconvoluted signals from different oxygen-containing moieties.

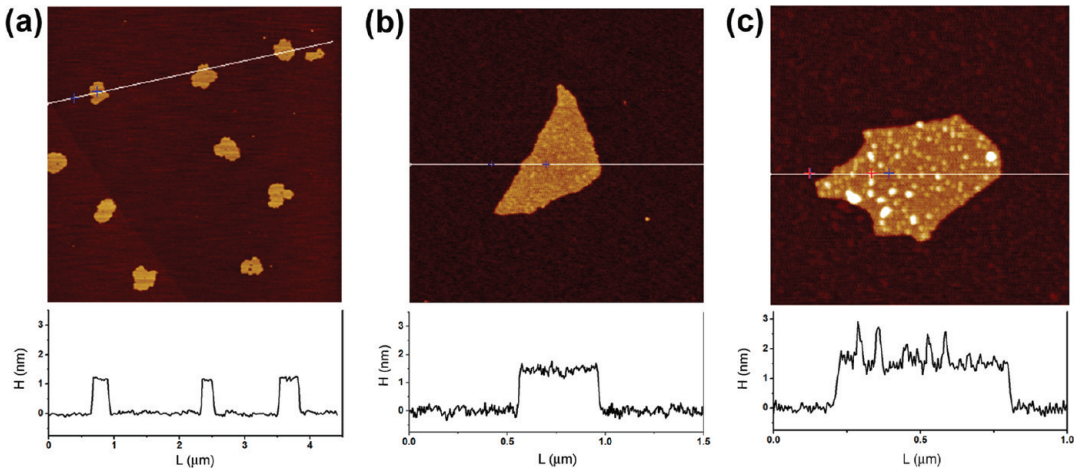

Figure 4. AFM height images of as-prepared graphene oxide sheets in the absence (a and b) and presence (c) of Pluronic 127 triblock copolymers (0.5 mM).

the as-prepared sheets (Figure 4) even though the level of oxygen functionalization has significantly increased. Together with the DLS data mentioned above, this observation suggests that the improved dispersibility (and cellular uptake, see discussion below) of doubly oxidized graphene oxide nanosheets can primarily be attributed to their highly oxidized structure and not their decreased size.

The enhanced stability of doubly oxidized graphene oxide dispersions, without the need for added surfactant, should circumvent the potential *in vivo* toxicity associated with surfactant materials (see Biomolecule Coupling and Cellular Uptake below). Furthermore, the lack of surface steric hindrance by stabilizers should facilitate the loading of larger amounts of biomolecular cargos to the fully exposed, doubly oxidized graphene oxide surface. Coupled to the large number of intrinsic oxygen-containing functional groups, such as carboxylic acid, hydroxyl, and epoxy groups, that are present on the surface of dougbly oxidized graphene oxide (*vide supra*), these characteristics should make graphene oxide an excellent biodelivery platform *via* increased biological functionalization, increased payload capacity, and increased cellular uptake (see Biomolecule Coupling and Cellular Uptake below).

Steric Stabilization with Pluronic F127. Although doubly oxidized graphene oxide exhibited enhanced electrostatic stability compared to the as-prepared material, some aggregation of these nanosheets was still observed after 2 h of exposure to solutions with NaCl concentrations ≥ 100 mM (Figure S3 in the SI). Because similarly high salt concentrations are often utilized in biological studies, a complementary strategy for stabilizing graphene oxide under these high-salt conditions is necessary if graphene oxide is to be used for a wider variety of biological applications. As mentioned above, steric stabilization of graphene oxide sheets against aggregation has been accomplished *via covalent functionalization* with a bulky surfactant.[4,10] We hypothesize that this cumbersome synthetic strategy might be replaced by a *noncovalent "coating"* of the graphene oxide sheet with the triblock copolymer Pluronic F127, which features a central hydrophobic PPO block that can interact strongly with residual aromatic regions on

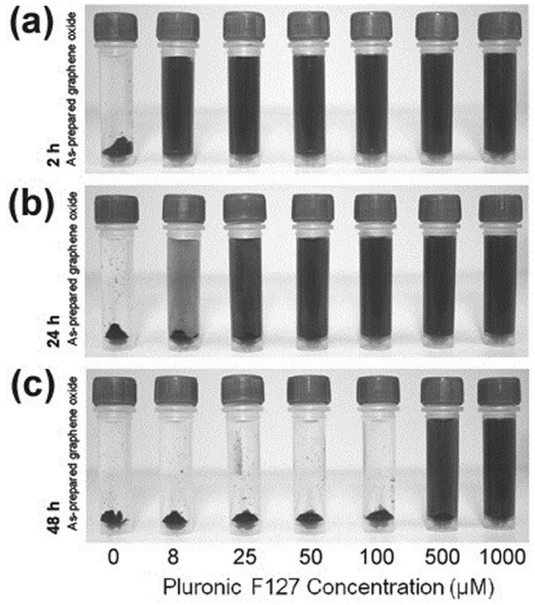

Figure 5. Digital images of solutions of as-prepared graphene oxide dispersions (0.1 mg mL^{-1}) taken after the addition of Pluronic F127 and incubation for (a) 2 h, (b) 24 h, and (c) 48 h in aqueous solutions of NaCl (75 mM). The concentrations of Pluronic F127 in the mixture are increased from left to right (0, 8, 25, 50, 100, 500, and 1000 μM) and are listed below the image. Samples were briefly centrifuged (~30 s) to accentuate the extent of aggregation of the nanosheet into concentrated masses at the bottom of the tube, if any. A color reproduction of this figure is available in the SI as Figure S8.

the graphene oxide basal plane and two sterically stabilizing hydrophilic PEG blocks that enhance aqueous solubility. Indeed, combining solutions of as-prepared graphene oxide with Pluronic F127 results in a homogeneous mixture that cannot be separated by centrifugation. Excellent adhesion of the copolymer to the as-prepared graphene oxide surface was confirmed *via* AFM, where the adsorbed polymer appears as white dots (<2.0 nm in height) on the basal plane of the nanosheets (Figure 4c and Figure S6 in the SI). In stark contrast, the AFM image of pristine graphene oxide did not exhibit any surface variance (Figures 4a,b and Figure S7 in the SI), with a consistent height of ~1.2 nm for all nanosheets. We note that having a long enough polymer chain, which can interact well with both the graphene oxide surface and the media, is important; an attempt to stabilize as-prepared graphene oxide with Pluronic F68, which is ~1/2 the length of Pluronic F127, resulted in faster aggregation in ionic media.

When added to aqueous NaCl solutions, solutions of Pluronic F127-coated graphene oxide exhibited excellent solubility in the presence of Na^+ and Cl^- ions up to 135 mM concentrations (Figure 2c). While relatively high concentrations of the surfactant copolymer (1 mM, 12.6 mg mL^{-1}) were originally employed to stabilize a typical graphene oxide nanosheet solution (0.1 mg mL^{-1}), much lower concentrations are also very effective. As little as 8 μM (0.1 mg mL^{-1}) concentration of copolymer can stabilize an equal mass of nanosheets (0.1 mg mL^{-1}) for a few hours in a 75 mM NaCl solution, with a slightly increased concentration (25 μM, 0.4 mg mL^{-1}) required for 24 h stability (Figure 5). However, high concentrations (>500 μM) of Pluronic F127 are necessary for long-term stability (>48 h). Indeed, after Pluronic F127 (final concentration = 1 mM) is added to a dispersion of as-prepared graphene oxide, the copolymer quickly "coats" the nanosheets (as evidenced by the increase of hydrodynamic radius to ~350 nm, Figure S2 in the SI), and the resulting Pluronic F127-stabilized nanosheets remained effectively unchanged in size after a 48 h incubation period in electrolyte solution (75 mM NaCl). We note that only as-prepared graphene oxide (*i.e.*, exposed to only one cycle of the Hummers oxidation) was utilized in this steric stabilization approach, as the doubly oxidized nanosheets described in the previous section did not interact well with the Pluronic F127 copolymer and exhibited limited enhancement in stability (Figure S9 in the SI). This is most likely due to a reduced interaction between the more oxidized nanosheet and the central PPO block of the surfactant copolymer: the very low C/O ratio (1.1) of the doubly oxidized material implies that the residual hydrophobic aromatic regions on the basal plane of the nanosheet, which interact the best with the PPO block, would be quite sparse and preclude the desired steric stabilization.

While amphiphilic copolymers, such as Pluronic F127, have been used to stabilize dispersions of graphene (C/O $\gg$ 100) prepared by direct sonication of graphite flakes,[28] as well as hydrazine-reduced graphene oxide (C/O $\approx$ 10),[26] the stabilization mechanism in these cases depends much more on the hydrophobic interactions between the copolymer surfactant and the graphene sheet than the as-prepared graphene oxide sheet in our case. Being more reduced, the aforementioned two materials are much more hydrophobic than our more hydrophilic[24] graphene oxides (C/O ratio = 1.1 for doubly oxidized graphene oxide and 1.9 for as-prepared graphene oxide) and should interact more strongly with the hydrophobic segment of Pluronic F127. Given the low C/O ratio in graphene oxide, and the consequently small total area of hydrophobic regions on the surface of these nanosheets, good interactions with the hydrophobic segment of Pluronic F127 were uncertain when we began our work. As mentioned above, Pluronic F127 does not interact well with doubly oxidized graphene oxide (C/O = 1.1) due to reduced interaction between its central hydrophobic block and these highly hydrophilic nanosheets.

Most notable is our observation that a very small amount of Pluronic F127 (100 wt %) can stabilize as-prepared graphene oxide in *75 mM aqueous NaCl*. This is in stark contrast to the excess amounts of amphiphilic block copolymers that have been used to disperse

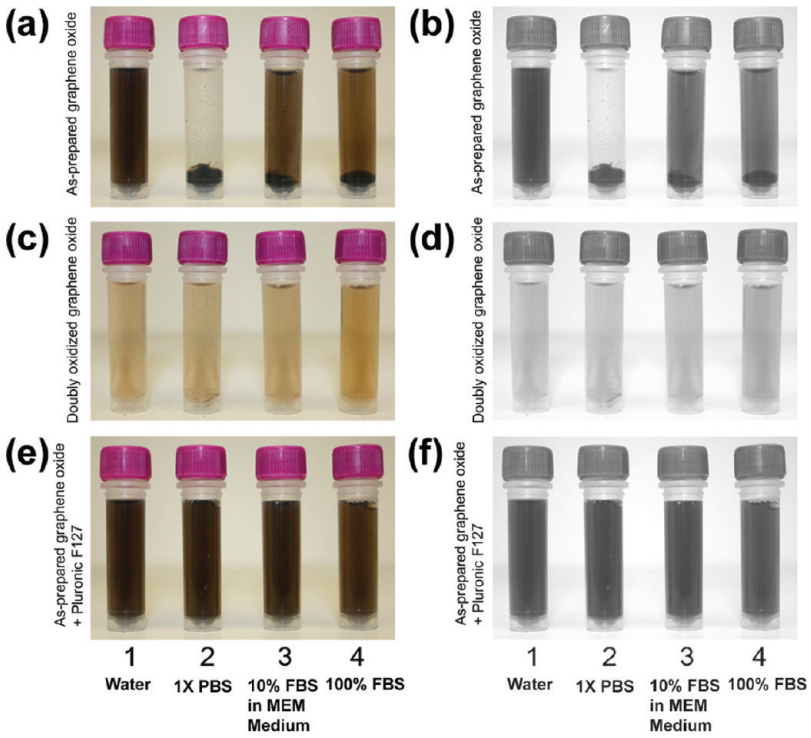

Figure 6. Digital images of solutions of (a and b) as-prepared graphene oxide (0.1 mg mL^{-1}) in different media, (c and d) doubly oxidized graphene oxide (0.1 mg mL^{-1}) in different media, and (e and f) as-prepared graphene oxide (0.1 mg mL^{-1}) in the presence of Pluronic F127 (1.0 mM) and different media. To accentuate contrast, the images in the right column are grayscale reproductions of those on the left. Images were recorded 5 min after the graphene oxide formulations were combined with the different media: (1) ultrapure deionized water, (2) 1× PBS, (3) 10% FBS in MEM cell culture medium, and (4) pure FBS. Samples were briefly centrifuged (~30 s) to accentuate the extent of aggregation of the nanosheet into concentrated masses at the bottom of the tube, if any.

graphene (14 200 wt %) and reduced graphene oxide (2700 wt %) *in pure water*.[26,28] Presumably, the increased hydrophilicity in our as-prepared graphene oxide can be translated into a lower requirement for Pluronic F127: the smaller total area of hydrophobic regions on the surface of as-prepared graphene oxide nanosheets, in comparison to those in graphene and reduced graphene oxide, would require less polymer for stabilization. As mentioned above, the lower surfactant requirement can be highly advantageous in delivery applications: the surfactant-associated *in vivo* toxicity can be decreased, while the surface area available for biofunctionalization and payload-tethering can be increased.

Biomolecule Coupling and Cellular Uptake. Solutions of electrostatically and sterically stabilized graphene oxide were diluted into a number of biological media to verify their suitability for delivery applications. As expected, both of our stabilization strategies yielded highly dispersed nanosheets in 1× PBS solution, 10% fetal bovine serum (FBS) in cell culture medium, and pure FBS (Figure 6) that are stable for several hours. Extended exposure for 24 h does not cause any aggregation of the Pluronic F127-coated graphene oxide. The doubly oxidized graphene oxide is also completely stable in pure FBS over this period; however, 1× PBS solution and 10% FBS in cell culture medium begin to induce some aggregation (Figure S10 in the SI).

Having successfully stabilized graphene oxide in biological media, we evaluated their ability to undergo conjugation with Cy3-labeled streptavidin through amide coupling to the carboxylic acid groups along the edge of the graphene oxide nanosheets. As a control, untreated as-prepared graphene oxide nanosheets were also subjected to the same streptavidin coupling procedure. Following the protein coupling, the nanosheets were filtered and washed with 1× PBS solution prior to assaying the amount of coupled streptavidin with UV−vis spectroscopy. The streptavidin-conjugated doubly oxidized and Pluronic F127-stabilized graphene oxide exhibited absorbances at 559 nm due to the Cy3 label, which were respectively 250% and 330% stronger than that for the protein-coupled, as-prepared nanosheets (Figure 7). These stronger absorbance values can be attributed to better dispersibilities in PBS solution afforded by our stabilization strategies, without which the nanosheets aggregated and could achieve only limited coupling with the streptavidins. The successful coupling of streptavidins with graphene oxide nanosheets was further confirmed by FTIR spectroscopy (Figure S12 in the SI1). Upon covalent coupling with a Cy3-labeled streptavidin, both FTIR spectra exhibit high-intensity amide I and II vibrational peaks.

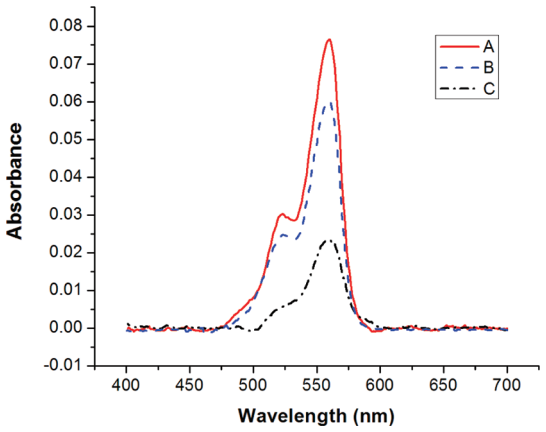

Figure 7. UV−vis spectra of graphene oxide solutions after covalent coupling (2 h reaction at room temperature) with Cy3-labeled streptavidin. After the coupling, the graphene oxide sheets were filtered and washed with 1× PBS solution to remove unbound molecules. A (red solid line): as-prepared graphene oxide in combination with Pluronic F127 coating. B (blue dashed line): doubly oxidized graphene oxide. C (black dash-dot line): as-prepared graphene oxide.

Analysis of the UV−vis data shows the amount of streptavidin loaded onto 1 mg samples of doubly oxidized and Pluronic F127-stabilized graphene oxide sheets to be 12.1 and 15.5 wt %, respectively. These values correspond to coupling yields of 30.4% and 38.8%; the higher yield for the Pluronic F127-stabilized material should be attributed to its higher stability against aggregation. In stark contrast, untreated graphene oxide can be loaded with only 4.5 wt % of streptavidin, equivalent to a coupling yield of 11.4%. As such, these studies demonstrate that electrostatic and steric stabilization are both viable strategies for producing homogeneous dispersions of graphene oxide with high loading capacities for biological applications.

To demonstrate the excellent potential of doubly oxidized and Pluronic F127-stabilized graphene oxide as delivery vehicles over unstabilized, as-prepared graphene oxide, we modified all three formulations with 5′-NH_2-terminated single-stranded oligodeoxyribonucleotides (ssODNs) and incubated the resulting materials with HeLa human cervical cancer cells. The ssODNs were also 3′-Cy3-labeled to provide a fluorescence signal that can be visualized with confocal laser-scanning microscopy (CLSM). While graphene oxide has previously been observed to quench the fluorescence of dyes that are attached close to the surface,[30] dye-labeled DNA duplexes have been found to exhibit only partially quenched signal when attached to graphene oxide,[31] as observed for our materials (Figure S13 in the SI). As expected, as-prepared graphene oxide exhibited more fluorescence quenching than doubly oxidized graphene oxide, presumably due to the presence of more residual graphitic domains in the basal plane of the former material.

CLSM images centered on the fluorescence of Cy3-labeled ssODNs showed no observable background

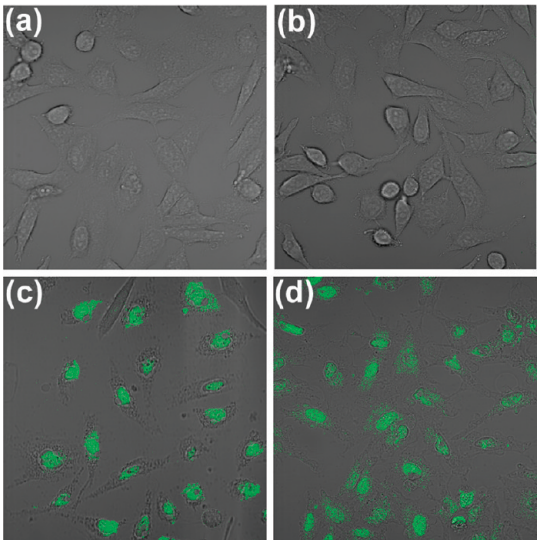

Figure 8. (a) Confocal laser scanning fluorescent microscopy (CLSM) image, centered on the fluorescence of Cy3, of HeLa cells shown as proof for the lack of background fluorescence in the blank sample. (b, c, and d) CLSM images, centered on the fluorescence of Cy3, of HeLa cells in fresh cell culture media after 2 h exposure to Cy3-labeled, ssODNs-coupled graphene oxide formulations: (b) as-prepared graphene oxide (1.7 μg mL^{-1}), (c) doubly oxidized graphene oxide (1.7 μg mL^{-1}), and (d) as-prepared graphene oxide (1.7 μg mL^{-1}) in the presence of Pluronic F127 (1 mM).

fluorescence from the starting HeLa cell (Figure 8a). However, cells that had been incubated with doubly oxidized and Pluronic F127-stabilized graphene oxide exhibited intense cytosolic fluorescence (Figure 8c and d, respectively). Such a strong signal indicates the efficient internalization of these stabilized nanosheets, a direct consequence of their good dispersity in cell culture media (Figure 6). This remarkably high cellular uptake is in stark contrast to that of the control (unstabilized, as-prepared) graphene oxide sample, where poor dispersibility in cell culture media induced clear aggregation *outside* of the cells (Figure S14a in the SI), precluding any uptake of the dye-labeled nanosheets into the HeLa cells (Figure 8b). Fluorescence intensity distribution plots (Figure S15 in the SI) and histograms (Figure S16 in the SI) of the CLSM images in Figure 8 provide a quantitative indication of the excellent cellular uptake efficiency of doubly oxidized and Pluronic F127-coated graphene oxide nanosheets: cell samples that have been exposed to these two materials exhibited ∼110 and ∼150 times higher fluorescence intensity per cell, respectively, in comparison to the cell sample that was exposed to untreated graphene oxide.

Notably, viability studies using HeLa cells demonstrate that doubly oxidized graphene oxide has a low *in vitro* cell toxicity (IC_{50} > 500 μg/mL based on extrapolation of available data in Figure S17 in the SI) that is similar to that for as-prepared graphene oxide, whose good biocompatibility has been reported by other research groups.[10,32] In contrast to literature reports[33,34]

that Pluronic F127 does not show *in vitro* cell toxicity at concentrations ≤ 4 mM, the [graphene oxide + Pluronic F127] mixture begins to exhibit some cell toxicity at ≥0.5 mM polymer concentration (Figure S17 in the SI). These observations suggest that the "coating" of graphene oxide by Pluronic F127 may have led to its enhanced uptake into the cells as the graphene oxide is being internalized; the result is a very different cytotoxicity profile than either of the two components. If this behavior proves to be general for other cell lines and organisms, the use of doubly oxidized graphene oxide as a carrier platform would indeed be complementary to Pluronic F127-stabilized graphene oxide, as it can eliminate some of the *in vivo* toxicity associated with increased usage of surfactants.

CONCLUSION

In summary, we have demonstrated two distinct and *complementary* strategies for enhancing the dispersibility of graphene oxide nanosheets in electrolyte aqueous solutions. In the first approach, the *electrostatic stability* of graphene oxide was greatly improved after a second cycle of Hummers oxidation, which lowers its C/O ratio from 1.9 to 1.1. The resulting doubly oxidized nanosheets featured a more negative zeta potential that allowed for excellent dispersion in biological media including PBS solution, 10% FBS in MEM cell culture medium, and pure FBS. This surfactant-free stabilization strategy greatly improves the promise of graphene oxide as a delivery vehicle by circumventing potential *in vivo* toxicity problems associated with the utilization of stabilizers and allowing for better functionalization/loading of biological payloads.

In the second strategy, *steric stability* was imbued to as-prepared graphene oxide by the addition of a small amount of the amphiphilic block copolymer Pluronic F127, whose central block interacted with residual hydrophobic, sp^2-hybridized regions on graphene oxide, while its terminal PEG chains served to stabilize the nanosheets in electrolyte-laden biological media. In contrast to previous reports,[26,28] where very large amounts of amphiphilic block copolymers were used to disperse only a small mass of *hydrophobic graphene* or *reduced graphene oxide* sheets in *pure water*, the *hydrophilic* nature of *graphene oxide* nanosheets enables a dramatic reduction in the mass of Pluronic F127 required for their stabilization *in the presence of a high concentration of electrolytes*. Most importantly, the great range of media dispersibility afforded by our two stabilization strategies allows the stabilized graphene oxide nanosheets to undergo highly efficient bioconjugation to proteins and nucleic acids in contrast to untreated graphene oxide. In addition, these stabilized nanosheets exhibited outstanding cellular uptake when incubated with HeLa cells, while the unstabilized nanosheets aggregated outside of the cells.

We stress that the electrostatic stabilization and the steric stabilization strategies reported herein should be viewed as *complementary* tools that can be used to improve the dispersibility of graphene oxide *in electrolyte solutions* for a wide variety of biological applications. These strategies improved upon a previously published approach[25] that focuses on stabilizing graphene oxide *in water*. Additionally, our strategies offer a facile means for improving the dispersibility of graphene oxide sheets in electrolyte solutions without the need to limit the size of these nanosheets or perform cumbersome postsynthesis covalent modification.[10]

The two stabilization strategies reported herein, coupled to the good biocompatibility of graphene oxide and its excellent surface-to-volume ratio, greatly expand the potential of graphene oxide nanosheets as a promising platform for the delivery of biomolecular payloads. It is indeed quite exciting to imagine the plethora of targeting ligands, imaging agents, and drug cargos that can be orthogonally attached to the wide variety of functional groups on the graphene oxide surface to create the next generation of multifunctional nanoscale drug-delivery systems. For such applications, the stabilization by Pluronic copolymers can potentially lead to enhanced uptake and reticuloendothelial system (RES)-shielding of graphene oxide nanosheets given the well-known ability of these copolymers to perturb the membrane structure[27] and protect against opsonization.[35,36] The results of these studies will be reported in due course.

MATERIALS AND METHODS

Materials. Graphite powder (SP-1) was used as received from Bay Carbon (Bay City, MI, USA). Unless otherwise noted, the terms as-prepared graphene oxide and singly oxidized graphene oxide are used interchangeably in this section for convenience. Cy3-labeled ssODNs (5′-amine-C6-CTTACGCTGAGTACTTCGATT-Cy3-3′) were obtained from Integrated DNA Technologies (Coralville, IA, USA). Cy3-labeled streptavidin was received from Invitrogen (Carlsbad, CA, USA). Pluronic F127, 1-(3-dimethylaminopropyl)-3-ethylcarbodiimide hydrochloride (EDC·HCl), *N*-hydroxysulfosuccinimide sodium salt (sulfo-NHS), PBS tablet for the preparation of PBS solution used in graphene oxide stabilization studies, and all other reagents were purchased from Sigma-Aldrich Chemical Co. (Milwaukee, WI, USA). Mica plates for AFM measurement were purchased from Ted Pella, Inc. (Redding, CA, USA). Ultrapure deionized water (18.2 MΩ cm resistivity) was obtained from a Millipore system (Billerica, MA, USA).

Characterization. Tapping-mode AFM experiments were performed with a Dimension Icon atomic force microscope (Bruker, CA, USA) using a TESPA tip from Veeco Corporation (Camarillo, CA, USA). In a typical experiment, graphene oxide dispersions in ultrapure deionized water (40 μL, 0.1 mg mL^{-1}) were dropped on a freshly cleaved mica plate. After 30 min incubation at room temperature, the plate was washed with ultrapure deionized water, dried at room temperature (5 min), and then further dried in an oven at 70 °C (30 min). The dried plate was stored in a clean Petri dish prior to AFM measurement.

UV−vis absorption spectra were obtained on a CARY 300 Bio UV−vis spectrophotometer (Varian Medical Systems, Inc., Palo Alto, CA, USA). Fluorescence emission spectra were obtained on a Jobin Yvon Fluorolog fluorometer (λ_{ex} = 549 nm, λ_{em} = 563 nm, slith width = 3 nm for Cy3). A confocal laser scanning microscope study was performed on a LSM 510 META microscope (Carl Zeiss MicroImaging, LLC, Thornwood, NY, USA).

DLS and zeta potential measurements were performed on a Zetasizer Nano ZS (Marvern Instruments, Malvern, UK) with a He−Ne laser (633 nm). Noninvasive backscatter method (detection at 173° scattering angle) was used. Correlation data were fitted, using the method of cumulants, to the logarithm of the correlation function, yielding the diffusion coefficient, D. The hydrodynamic diameters (D_H) of graphene oxide nanosheets were calculated using D and the Stokes−Einstein equation ($D_H = k_BT/3\pi\eta D$, where k_B is the Boltzmann constant, T is the absolute temperature, and η is the solvent viscosity (η = 0.8872 cP for water)). The reported data represent an average of eight measurements with 10 scans each.

XPS spectra were collected in the Keck II/NUANCE facility at Northwestern University (NU) with an Omicron (Taunusstein, Germany) ESCA Probe (Al Kα radiation, $h\nu$ = 1486.6 eV). A Shirley background was removed from atomic spectra prior to deconvolution. FTIR spectroscopy was performed at the KECK-II/NUANCE facility at NU using a Nexus 870 spectrometer (Thermo Nicolet, West Palm Beach, FL, USA). Samples were ground together with KBr and pressed into a pellet for data collection in transmission mode. Elemental analysis was performed by Atlantic Microlabs (Norcross, GA, USA).

Solid-state ^{13}C MAS NMR spectra were collected in the IMSERC facility at NU on a Varian VNMRS 400 MHz solid-state NMR spectrometer (equipped with an HXY triple-resonance probe tuned to ^1H and ^{13}C, Varian Instruments, Inc., Santa Clara, CA, USA) with proton decoupling. Relaxation delays of 60 s and a MAS rate of 10 000 Hz were used for all samples. Chemical shifts were determined against an external adamantane standard and are reported relative to tetramethylsilane (0 ppm).

Preparation of Graphene Oxide Sheets. Graphite was oxidized to graphite oxide using a modification of the Hummers method.[29] A 500 mL round-bottom flask was loaded with a large Teflon-coated magnetic stir bar, graphite (5 g), $NaNO_3$ (2.5 g), and concentrated H_2SO_4 (115 mL) and then stirred vigorously to combine. After dissolution of the sodium nitrate, the flask was cooled in an ice bath, and solid $KMnO_4$ (15 g) was added slowly with stirring over 10 min to prevent dangerous overheating (*i.e.*, >30 °C). Upon addition of all $KMnO_4$, the ice bath was replaced with a water bath (35 °C) and the solution was stirred vigorously for 3 h. During this time, the solution became highly viscous and turned dark brown. The reaction flask was then cooled in an ice/salt bath, and ultrapure deionized water (230 mL) was slowly added to the solution, ensuring that the temperature remained below 40 °C. The resulting diluted brown mixture was poured into ultrapure deionized water (700 mL) and quenched with hydrogen peroxide (12 mL), yielding a light yellow suspension of graphite oxide. The resulting graphite oxide was purified by three cycles of centrifugation (8230*g* for 5 min in a model 5804R centrifuge (Eppendorf, Westbury, NY, USA)), decantation, and resuspension in 4 wt % aqueous HCl solution. This three-cycle process was then repeated with ultrapure deionized water to generate purified graphite oxide.

The as-synthesized purified graphite oxide was suspended in ultrapure deionized water (500 mL) and exfoliated into individual graphene oxide nanosheets using a titanium-alloy solid probe ultrasonicator (500 W Vibra-Cell VC 505, Sonics & Materials, Inc., Newtown, CT, USA) set at 30% intensity with 10 s/10 s ON/OFF pulses and a total of 2 h ON time. Any residual unexfoliated graphite oxide was removed by centrifugation at 8230*g* for 5 min with the precipitate discarded. The resulting graphene oxide solution was then dialyzed in ultrapure deionized water to remove remaining salts (4 × 5 L, with water changed every 4 h during daytime or after overnight).

Double Oxidation of Graphene Oxide. An aqueous dispersion of as-prepared graphene oxide was lyophilized (FreeZone 1Liter Benchtop, Labconco, Corp., Kansas City, MO, USA) to remove all water. The resulting dried graphene oxide sample (0.4 g) was then subjected once more to the modified Hummers oxidation (see above) with proper scaling of all other reagents. All operations were repeated as described above to yield doubly oxidized graphene oxide.

Stabilizing with Pluronic F127. An appropriate amount of a stock solution of Pluronic F127 (5 mM in water) was added to an aqueous dispersion of as-prepared graphene oxide (prepared from a parent dispersion (1.0 mg mL^{-1}) that has been diluted with ultrapure deionized water) to provide the appropriate formulations. The mixture was vortexed (S/P Vortex Mixer (Charlotte, NC, USA)) briefly (~10 s) to ensure homogeneous distribution of both components.

Coupling of Streptavidin to Graphene Oxide Sheets. In Eppendorf tubes, aqueous dispersions of the appropriate graphene oxide formulations (250 μL, 0.2 mg mL^{-1}) were mixed with 2× PBS solution (250 μL) to create mixtures with 1× PBS strength. The solutions were vortexed briefly before and after the addition of EDC·HCl (1.0 mg) and sulfo-NHS (1.5 mg). After 30 min incubation, the solutions were filtered with an Amicon Ultra centrifugal filter (100K MWCO, Millipore) *via* centrifugation at 14000*g* for 30 min. The filtered graphene oxide sheets were then washed with water (3 × 400 μL) *via* centrifugation at 14000*g* for 30 min. The isolated graphene oxide sheets were redispersed in 1× PBS solution (200 μL), combined with either Cy3-labeled streptavidin (20 μL, 1 mg mL^{-1}) or a mixture of Cy3-labeled streptavidin (20 μL, 1 mg mL^{-1}) and Pluronic F127 (50 μL of a 5 mM solution), and vortexed to homogeneity. After incubation in the dark at room temperature for 2 h, the resulting solutions were filtered with an Amicon Ultra centrifugal filter (100K MWCO) *via* centrifugation at 14000*g* for 30 min before washing with 1× PBS solution (4 × 400 μL) *via* centrifugation at 14000*g* for 30 min. The amount of streptavidin coupled to the collected graphene oxide sheets was determined by measuring the UV−vis absorbance of the Cy3 dye tag on the streptavidin. As the filtration process removed <10% of the original graphene oxide sheets (see Figure S18 in the SI), the mass of the collected graphene oxide sheets was assumed to be unchanged for calculation purposes.

Coupling of ssODNs with Graphene Oxide Sheets for CLSM Study. Aqueous dispersions of the appropriate graphene oxide formulations (50 μL, 1.0 mg mL^{-1}) were diluted to 190 μL with ultrapure deionized water. EDC·HCl (1.0 mg), sulfo-NHS (1.5 mg), and Cy3-labeled ssODN (10 μL of a 200 μM stock solution) were then added, and the resulting mixture was vortexed briefly before being incubated in the dark at room temperature for 2 h. After incubation, the reaction mixture then filtered with an Amicon Ultra centrifugal filter (100K MWCO, Millipore) *via* centrifugation at 14000*g* for 30 min. The filter was then washed with ultrapure deionized water (5 × 400 μL) *via* centrifugation at 14000*g* for 30 min.

Following the procedure described above, two different graphene oxide samples (doubly oxidized graphene oxide and as-prepared graphene oxide) were coupled to Cy3-labeled ssODNs. The corresponding DNA-coupled Pluronic F127-stabilized sample was then prepared by mixing an appropriate amount of Pluronic F127 with the Cy3-labeled, ssODNs-coupled as-prepared graphene oxide sample.

Cell Culture. *a. Media and Cell Culture Reagents.* All Corning-brand cell culture consumables (flasks, plates, and pipettes) were purchased from Fisher Scientific (Pittsburgh, PA, USA). Minimum essential medium (MEM), FBS, and trypsin solutions were purchased from Invitrogen (Carlsbad, CA, USA). Media were kept antibiotic-free through use of sterile techniques, and all reagents were phenol red-free. The 1× PBS solution for cell washing was purchased from Mediatech (Manassas, VA, USA).

b. Cell Line and Conditions. HeLa human cervical cancer cells (CCL-2) were purchased from American Type Culture Collection (ATCC, Manassas, VA, USA). HeLa cells were cultured using MEM supplemented with 10 vol % FBS at 37 °C in an incubator equipped with a humidified atmosphere containing 5 vol % CO_2. HeLa cells were harvested using a 0.05 vol % trypsin solution.

Confocal Laser Scanning Microscopy Imaging. Eight-well chambered cover glasses were purchased from Fisher Scientific (Pittsburgh, PA, USA) for culturing and viewing living cells *via*

CLSM. Before each experiment, HeLa cells were planted in MEM (200 μL) in the eight-well chambered cover glasses and placed in an incubator equipped with a humidified atmosphere containing 5 vol % CO_2 at 37 °C for 24 h. Fresh MEM (200 μL) was then added, and the cells were then incubated in the same chamber together with the appropriate formulation of Cy3-labeled, ssODNs-coupled graphene oxide (1.7 μg mL^{-1}), with or without Pluronic F127 (1 mM final concentration), at 37 °C for 2 h. After the removal of the graphene oxide-containing medium, the cell layers were washed with 1× PBS solution (3 × 200 μL) and fresh MEM (200 μL) was added. CLSM images were collected with an excitation wavelength of 543 nm (He−Ne laser) using a water-immersion objective (C-Apochromat 40×/1.20 W Korr). Obtained images were converted to TIFF format with ZEN 2009 software (Carl Zeiss MicroImaging, LLC).

Cytotoxicity Assay. HeLa cells (~4000 cells/well) were plated into 96-well plates, and then preprepared media containing desired concentrations of graphene oxide samples were added to each well. After incubation for 48 h, the cells were washed with fresh MEM (2 × 100 μL), and then cell viability was measured *via* an MTS cell-proliferation assay. The relative cell-survival percentages compared to the graphene oxide-free control were plotted against the graphene oxide concentration in logarithmic scale. The reported data represent averages and error bars of three measurements from different batches.

Acknowledgment. This work is financially supported by the NIH (NCI Center of Cancer Nanotechnology Excellence Grant C54CA151880, and Core Grant P30CA060553 to the Robert H. Lurie Comprehensive Cancer Center of Northwestern University). O.C.C. is an ACC-NSF fellow (CHE-0936924). Z.A. is supported by the ARO (Award # W991NF-09-1-0541) and a Ryan Fellowship. I.E. is supported by the NSF (Grant EEC-0647560 through the NSEC program).

Supporting Information Available: Solid-state ^{13}C NMR spectra of as-prepared and doubly oxidized graphene oxide, cell viability and DLS data, calibration curves, FTIR and fluorescence spectra, fluorescence intensity distribution images and histogram, and additional dispersion, AFM, and CLSM images. This material is available free of charge *via* the Internet at http://pubs.acs.org.

REFERENCES AND NOTES

1. Lerf, A.; He, H.; Forster, M.; Klinowski, J. Structure of Graphite Oxide Revisited. *J. Phys. Chem. B* **1998**, *102*, 4477–4482.
2. Cai, W.; Piner, R. D.; Stadermann, F. J.; Park, S.; Shaibat, M. A.; Ishii, Y.; Yang, D.; Velamakanni, A.; An, S. J.; Stoller, M.; *et al.* Synthesis and Solid-State NMR Structural Characterization of ^{13}C-Labeled Graphite Oxide. *Science* **2008**, *321*, 1815–1817.
3. Stankovich, S.; Piner, R. D.; Nguyen, S. T.; Ruoff, R. S. Synthesis and Exfoliation of Isocyanate-Treated Graphene Oxide Nanoplatelets. *Carbon* **2006**, *44*, 3342–3347.
4. Niyogi, S.; Bekyarova, E.; Itkis, M. E.; McWilliams, J. L.; Hamon, M. A.; Haddon, R. C. Solution Properties of Graphite and Graphene. *J. Am. Chem. Soc.* **2006**, *128*, 7720–7721.
5. Erickson, K.; Erni, R.; Lee, Z.; Alem, N.; Gannett, W.; Zettl, A. Determination of the Local Chemical Structure of Graphene Oxide and Reduced Graphene Oxide. *Adv. Mater.* **2010**, *22*, 4467–4472.
6. Becerril, H. A.; Mao, J.; Liu, Z.; Stoltenberg, R. M.; Bao, Z.; Chen, Y. Evaluation of Solution-Processed Reduced Graphene Oxide Films as Transparent Conductors. *ACS Nano* **2008**, *2*, 463–470.
7. Cote, L. J.; Kim, F.; Huang, J. Langmuir-Blodgett Assembly of Graphite Oxide Single Layers. *J. Am. Chem. Soc.* **2009**, *131*, 1043–1049.
8. Compton, O. C.; Nguyen, S. T. Graphene Oxide, Highly Reduced Graphene Oxide, and Graphene: Versatile Building Blocks for Carbon-Based Materials. *Small* **2010**, *6*, 711–723.
9. Liu, Y.; Yu, D.; Zeng, C.; Miao, Z.; Dai, L. Biocompatible Graphene Oxide-Based Glucose Biosensors. *Langmuir* **2010**, *26*, 6158–6160.
10. Liu, Z.; Robinson, J. T.; Sun, X.; Dai, H. PEGylated Nanographene Oxide for Delivery of Water-Insoluble Cancer Drugs. *J. Am. Chem. Soc.* **2008**, *130*, 10876–10877.
11. Chen, H.; Müller, M. B.; Gilmore, K. J.; Wallace, G. G.; Li, D. Mechanically Strong, Electrically Conductive, and Biocompatible Graphene Paper. *Adv. Mater.* **2008**, *20*, 3557–3561.
12. Jung, J. H.; Cheon, D. S.; Liu, F.; Lee, K. B.; Seo, T. S. A Graphene Oxide Based Immuno-Biosensor for Pathogen Detection. *Angew. Chem., Int. Ed.* **2010**, *49*, 5708–5711.
13. Shen, J.; Shi, M.; Yan, B.; Ma, H.; Li, N.; Hu, Y.; Ye, M. Covalent Attaching Protein to Graphene Oxide Via Diimide-Activated Amidation. *Colloids Surf., B* **2010**, *81*, 434–438.
14. Zuo, X.; He, S.; Li, D.; Peng, C.; Huang, Q.; Song, S.; Fan, C. Graphene Oxide-Facilitated Electron Transfer of Metalloproteins at Electrode Surfaces. *Langmuir* **2010**, *26*, 1936–1939.
15. Lu, C.-H.; Yang, H.-H.; Zhu, C.-L.; Chen, X.; Chen, G.-N. A Graphene Platform for Sensing Biomolecules. *Angew. Chem., Int. Ed.* **2009**, *48*, 4785–4787.
16. He, S.; Song, B.; Li, D.; Zhu, C.; Qi, W.; Wen, Y.; Wang, L.; Song, S.; Fang, H.; Fan, C. A Graphene Nanoprobe for Rapid, Sensitive, and Multicolor Fluorescent DNA Analysis. *Adv. Funct. Mater.* **2010**, *20*, 453–459.
17. Liu, F.; Choi, J. Y.; Seo, T. S. Graphene Oxide Arrays for Detecting Specific DNA Hybridization by Fluorescence Resonance Energy Transfer. *Biosens. Bioelectron.* **2010**, *25*, 2361–2365.
18. Wang, Y.; Li, Z.; Hu, D.; Lin, C.-T.; Li, J.; Lin, Y. Aptamer/Graphene Oxide Nanocomplex for *in Situ* Molecular Probing in Living Cells. *J. Am. Chem. Soc.* **2010**, *132*, 9274–9276.
19. Sun, X.; Liu, Z.; Welsher, K.; Robinson, J. T.; Goodwin, A.; Zaric, S.; Dai, H. Nano-Graphene Oxide for Cellular Imaging and Drug Delivery. *Nano Res.* **2008**, *1*, 203–212.
20. Yang, X.; Zhang, X.; Liu, Z.; Ma, Y.; Huang, Y.; Chen, Y. High-Efficiency Loading and Controlled Release of Doxorubicin Hydrochloride on Graphene Oxide. *J. Phys. Chem. C* **2008**, *112*, 17554–17558.
21. Zhang, L.; Lu, Z.; Zhao, Q.; Huang, J.; Shen, H.; Zhang, Z. Enhanced Chemotherapy Efficacy by Sequential Delivery of siRNA and Anticancer Drugs Using PEI-Grafted Graphene Oxide. *Small* **2011**, *7*, 460–464.
22. Wang, X.; Zhi, L.; Müllen, K. Transparent, Conductive Graphene Electrodes for Dye-Sensitized Solar Cells. *Nano Lett.* **2008**, *8*, 323–327.
23. Park, S.; An, J.; Jung, I.; Piner, R. D.; An, S. J.; Li, X.; Velamakanni, A.; Ruoff, R. S. Colloidal Suspensions of Highly Reduced Graphene Oxide in a Wide Variety of Organic Solvents. *Nano Lett.* **2009**, *9*, 1593–1597.
24. Kim, J.; Cote, L. J.; Kim, F.; Yuan, W.; Shull, K. R.; Huang, J. Graphene Oxide Sheets at Interfaces. *J. Am. Chem. Soc.* **2010**, *132*, 8180–8186.
25. Li, D.; Müller, M. B.; Gilje, S.; Kaner, R. B.; Wallace, G. G. Processable Aqueous Dispersions of Graphene Nanosheets. *Nat. Nanotechnol.* **2008**, *3*, 101–105.
26. Zu, S.-Z.; Han, B.-H. Aqueous Dispersion of Graphene Sheets Stabilized by Pluronic Copolymers: Formation of Supramolecular Hydrogel. *J. Phys. Chem. C* **2009**, *113*, 13651–13657.
27. Batrakova, E. V.; Kabanov, A. V. Pluronic Block Copolymers: Evolution of Drug Delivery Concept from Inert Nanocarriers to Biological Response Modifiers. *J. Controlled Release* **2008**, *130*, 98–106.
28. Seo, J.-W. T.; Green, A. A.; Antaris, A. L.; Hersam, M. C. High-Concentration Aqueous Dispersions of Graphene Using Nonionic, Biocompatible Block Copolymers. *J. Phys. Chem. Lett.* **2011**, *2*, 1004–1008.
29. Hummers, W. S.; Offeman, R. E. Preparation of Graphitic Oxide. *J. Am. Chem. Soc.* **1958**, *80*, 1339–1339.
30. Kim, J.; Cote, L. J.; Kim, F.; Huang, J. Visualizing Graphene Based Sheets by Fluorescence Quenching Microscopy. *J. Am. Chem. Soc.* **2010**, *132*, 260–267.
31. Mohanty, N.; Berry, V. Graphene-Based Single-Bacterium Resolution Biodevice and DNA Transistor: Interfacing

Graphene Derivatives with Nanoscale and Microscale Biocomponents. *Nano Lett.* **2008**, *8*, 4469–4476.
32. Wang, K.; Ruan, J.; Song, H.; Zhang, J.; Wo, Y.; Guo, S.; Cui, D. Biocompatibility of Graphene Oxide. *Nanoscale Res. Lett.* **2011**, *6*, doi: 10.1007/s11671-11010-19751-11676.
33. Khattak, S. F.; Bhatia, S. R.; Roberts, S. C. Pluronic F127 as a Cell Encapsulation Material: Utilization of Membrane-Stabilizing Agents. *Tissue Eng.* **2005**, *11*, 974–983.
34. Exner, A. A.; Krupka, T. M.; Scherrer, K.; Teets, J. M. Enhancement of Carboplatin Toxicity by Pluronic Block Copolymers. *J. Controlled Release* **2005**, *106*, 188–197.
35. Jackson, J. K.; Springate, C. M. K.; Hunter, W. L.; Burt, H. M. Neutrophil Activation by Plasma Opsonized Polymeric Microspheres: Inhibitory Effect of Pluronic F127. *Biomaterials* **2000**, *21*, 1483–1491.
36. Owens, D. E., III; Peppas, N. A. Opsonization, Biodistribution, and Pharmacokinetics of Polymeric Nanoparticles. *Int. J. Pharmaceut.* **2006**, *307*, 93–102.